

COMPETITION BETWEEN HYDROGEN BONDING AND HALOGEN BONDING INTERACTIONS: ICN-H₂S SYSTEM

Dipali Singh

*A dissertation submitted for the partial
fulfilment of BS-MS dual degree in science*



Indian Institute of Science Education and Research Mohali
April 2019

Certificate of Examination

This is to certify that the dissertation titled “Competition between Hydrogen bonding and Halogen Bonding: ICN-H₂S System” submitted by Ms. Dipali Singh (MS14109) for the partial fulfilment of BS-MS dual degree program of the Institute, has been examined by the thesis committee duly appointed by the Institute. The committee finds the work done by the candidate satisfactory and recommends that the report be accepted.

Dr. P. Balanarayan

Dr. S. Venkataramani

Prof. K. S. Viswanathan

(Supervisor)

Dated: 26 April, 2019

Declaration

The work presented in this dissertation has been carried out by me under the guidance of Dr. K. S. Viswanathan at the Indian Institute of Science Education and Research Mohali.

This work has not been submitted in part or in full for a degree, a diploma, or a fellowship to any other university or institute. Whenever contributions of others are involved, every effort is made to indicate this clearly, with due acknowledgement of collaborative research and discussions. This thesis is a bonafide record of original work done by me and all sources listed within have been detailed in the bibliography.

Dipali Singh
MS14109

Dated: April 26, 2019

In my capacity as the supervisor of the candidate's project work, I certify that the above statements by the candidate are true to the best of my knowledge.

Prof. K. S. Viswanathan
(Supervisor)

Acknowledgement

I would like to express my gratitude towards my teacher and my guide Prof. K. S. Viswanathan for allowing me to work on the project of my interest. I thank him for his constant guidance and in valued support throughout the project. I would thank all my lab members especially MR. Pankaj Dubey and Ms. Jyoti Saini for constantly helping me and correcting me whenever required. Without their opinions and extended support, the project would not have been the same.

I want to acknowledge the guidance of all my committee members Dr. P. Balanarayana and Dr. R. Sugumar Venkataramani for their valuable suggestions and discussions.

I also acknowledge all my friends who always remain with me through all the times, Shakshi, Naman, Prateek, Prabhat, Komal, Kaveri, Anupreet, Neeraj, Ankuj, Sukhpal, Renu for being a special part of my journey and to bear with me whenever I was preposterous.

Last but not least, I would like to thank my family: my parents Mr. Baljit Singh and Mrs. Seema for being a constant source of motivation and inspiration. I thank them for being there, always.

I have no valuable words to express my thanks, but my heart is full of favors received from every person.

Dipali

List of Figures

Figure	Figure Caption	Page No.
1.1	Hydrogen bonding in water.	1
1.2	Halogen bond (acceptor and donors).	2
1.3	Image showing formation of positive σ -hole regions at halogen atoms along the C---X bond.	2
1.4	σ -Hole region formed over Iodine in ICN.	3
1.5	Interaction of Pi-cloud over benzene with lone pair.	3
2.1	(a) The general schematic diagram for the cryo-system assembly; (b) The schematic for the cryostat head mounted on the FTIR Spectrophotometer; (c) Picture of the cryostat mounted in Matrix Isolation set up at IISER Mohali.	8
2.2	Mixing chamber (Stainless steel).	9
3.1	Local and global minimum at potential energy surface.	13
4.1	σ -hole character of ICN.	17
4.2	Electron density topologies a) Halogen Interaction. b) Hydrogen Interaction. (BCPs corresponding to these interactions are circled)	19
4.3	FTIR spectra of H ₂ S in the symmetric stretch region. Experimental spectrum of A) ICN in an Ar matrix, B) H ₂ S in an Ar matrix, C) ICN-H ₂ S in Ar (ICN at 0°C) at 12K, D) ICN-H ₂ S in Ar annealed at 30K, Computed spectra of ICN-H ₂ S, E) Hydrogen bonded complex, F) Halogen bonded complex.	22
4.4	FTIR spectra of ICN in the CN stretch region Experimental spectrum of A) ICN in an Ar matrix, B) H ₂ S in an Ar matrix, C) ICN-H ₂ S in Ar (ICN at 0°C) at 12K, D) ICN-H ₂ S in Ar annealed at 30K, Computed spectra of ICN-H ₂ S, E) Hydrogen bonded complex, F) Halogen bonded complex.	23
4.5	Electron density topologies for the ICN-CH ₃ SH a) Halogen bonded and b) Hydrogen bonded complexes at the M06-2X/DGDZVP level.	25
4.6	Comparison of ICN-H ₂ O and ICN-H ₂ S system with their RAW/ZPE corrected/BSSE corrected interaction energies in kcal/mol at M06-2X/DGDZVP level.	26
4.7	Comparison of ICN-CH ₃ OH and ICN-CH ₃ SH system with their RAW/ZPE corrected/BSSE corrected interaction energies in kcal/mol at M06-2X/DGDZVP level.	27

List of Tables

Tables	Tables Caption	Page No.
4.1	Energies for halogen, hydrogen and pi-cloud interaction at different levels of theories.	18
4.2	AIM results showing the charge density and Laplacian for interactions on BCP at M06-2X/DGDZVP level.	19
4.3	NBO analysis showing some important donor and acceptor orbital interactions for ICN-H ₂ S complexes. E denotes delocalization energy in kcal/mol for each interaction.	20
4.4	Computed scaled vibrational frequencies (in cm ⁻¹) with their shifts calculated as $\nu_{\text{complex}} - \nu_{\text{monomer}}$ at M06-2X/DGDZVP level.	21
4.5	Interaction energies for Halogen and Hydrogen bonded ICN-CH ₃ SH complexes at different levels of theories.	24
4.6	Charge Density and Laplacian for Interactions at M06-2X/DGDZVP level of theory (in a.u).	25

Notations

AIM : Atom in Molecule

BCP : Bond Critical Point

RCP : Ring Critical Point

NBO : Natural Bonding Orbital

NAO : Natural Atomic Orbital

NHO : Natural Hybrid Orbital

DFT : Density Function Theory

HF : Hartree Fock

B3LYP : Becke-Lee-Yang-Parr

M06-2X : Mixed HF (2X refers to the percent of HF exchanged)

MP2 : Moller Plesset Perturbation Theory

ZPE : Zero Point Energy

BSSE : Basis Set Superposition Error

Contents

	List of Figures	i
	List of Tables	iii
	Notations	v
	Abstract	ix
Chapter 1	Introduction	1
1.1	Hydrogen bonding interaction	1
1.2	Halogen bonding interactions	1
1.3	Pi-cloud interactions	3
Chapter 2	Experimental Methods	5
2.1	Matrix Isolation FTIR Spectroscopy	5
2.1.1	Advantages	5
2.1.2	Properties of Matrix	6
2.2	Matrix Isolation FTIR Instrumentation	6
2.2.1	Cryostat	8
2.2.2	Vacuum system	9
2.2.3	FTIR spectrometer	9
2.2.4	Sample introduction system	9
Chapter 3	Computational Procedure	12
3.1	Computational Methods	12
3.1.1	<i>Ab initio</i> studies	12
3.2	Energy Calculations	12
3.2.1	Geometry optimization	13
3.2.2	Stabilization energies	13
3.3	Analysis of Different Weak Complexes	14
3.3.1	Atom in molecule (AIM) analysis methodology	15
3.3.2	Natural bonding orbital (NBO) analysis	15
Chapter 4	Results and Discussions	17
4.1	H ₂ S- ICN Complexes	17
4.1.1	Computational results	17
4.1.2	Atom in molecule (AIM) analysis	18
4.1.3	Experimental results	20
4.2	CH ₃ SH- ICN Complexes	23
4.2.1	Computational studies	24
4.2.2	Atom in molecule (AIM) analysis	25
4.3	Comparison	25
Chapter 5	Conclusions	29
	Bibliography	30

Abstract

Iodine attached to strongly electron withdrawing group can manifest halogen bonding interaction. In this study, we have examined the ICN molecule for its ability to show halogen bonding; the strong electron withdrawing CN group leads to the formation of σ -hole. Interestingly, ICN can also show hydrogen bonding interactions through nitrogen atom and therefore present the possibility of competitive bonding between the two types of non-covalent interactions – hydrogen and halogen bonding. We have studied this competitive binding with H₂S as the partner molecule.

The studies have been done on two systems; one is H₂S-ICN and CH₃SH-ICN. Three types of interactions were seen computationally; halogen bonding, hydrogen bonding and the interaction of S of H₂S with pi-cloud of the CN triple bond. Experimentally however we observed evidence only for the hydrogen bonding, even though the halogen bonding was found to be more strongly bound. A comparison of these results have also been made with the corresponding oxygen counterpart; i.e., ICN-H₂O system.

CHAPTER 1

INTRODUCTION

Intermolecular forces are forces of attraction or repulsion between molecules and atoms. The intermolecular interactions are non-covalent and stabilize molecular complexes composed of two or more different molecules. The non-covalent interactions is the ability of covalently bonded atoms in a molecule to participate in the different form of weak interactions with other molecules. There are mainly four types of non-covalent interactions, hydrogen bonding interaction, ionic-bonding interactions, van der Waals interactions, and hydrophobic interactions. The strength of such non-covalent interactions ranges from 1 kcal/mol to 40 kcal/mol. Owing to this range in the energy, non-covalent interaction provides the ability to associate and dissociate easily at room temperature conditions.

1.1 Hydrogen Bonding Interactions:

Hydrogen bonding interaction is a dipole-dipole interaction which involves interaction between the partially positive hydrogen atom and a highly electronegative atom. Most common atoms which can form hydrogen bonds easily are Fluorine, Oxygen and Nitrogen. The strength of a Hydrogen bond usually lies between 14 kcal/mol to 40 kcal/mol. The strength of hydrogen bonding interaction is significantly stronger than an ordinary dipole-dipole interaction^[1]. Hydrogen bonds have about a tenth of the strength of an average covalent bond and are being constantly broken and reformed in liquid water. The hydrogen bonding in water is shown in figure 1.1.

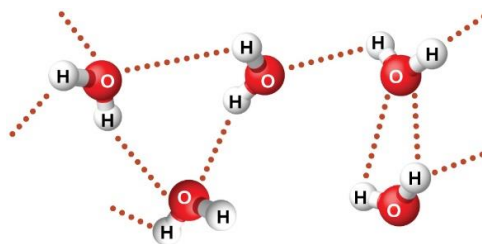


Figure 1.1: Hydrogen bonding in water. ^[2]

1.2 Halogen Bonding Interactions:

Halogen bonding is also a dipole-dipole interaction, in which. Halogen atom acts as an electrophile and interacts electrostatically with an electron rich species (nucleophile).

Generally, the nucleophilic agent in these interactions is more electronegative such as fluorine, oxygen, nitrogen, and sulfur. Halogens participating in halogen bonding interactions include Iodine, Bromine, Chlorine, and sometimes Fluorine. These halogens are capable of acting as XB donors and follow the general trend: $F < Cl < Br < I$, with iodine normally forming the strongest interactions. Figure 1.2. Shows the basic idea for a Halogen bond acceptors and donors.

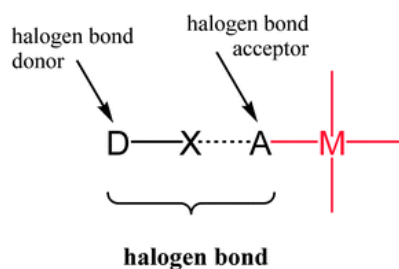


Figure 1.2: Halogen bond (acceptor and donors.)^[3]

A surprising feature of Halogen bond is that a halogen atom which generally concerned with having negative charges is viewed as an electron donor in this case. This possible explanation for this was supposed to be the positive region of halogen atom along the Carbon axis, as shown in Figure 1.3.

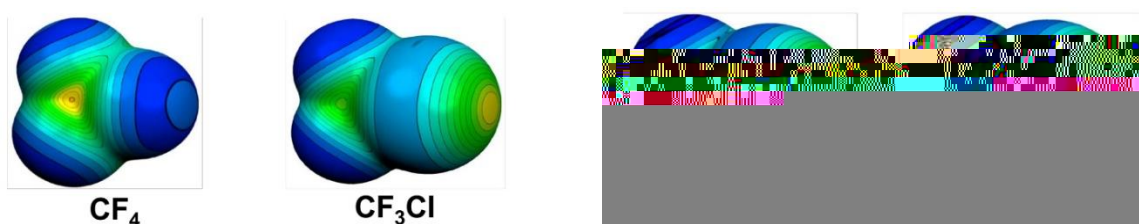


Figure 1.3. Image showing formation of positive σ -hole regions at halogen atoms along the C---X bond.^[4]

It is clear from the figure 1.3. above that the positive region formed in Iodine is the strongest among the three followed by Bromine, Chlorine, and Fluorine. The explanation for that is the size of Iodine atom which is large thus in it the outer shell electrons are farthest from nuclei. This feature thus helps the Iodine atom to act as an electron donor and thus forming halogen bonds easily. This positive region seen on the Halogen atom is called the σ -hole

region.

The studies on Halogen bonding in our study focuses on the σ -hole region formed over Iodine in ICN as Iodine can be taken as an ideal atom to show aspects of Halogen bonding because of its bigger size^[5]. The σ -hole region formed over Iodine in ICN is shown in figure 1.4.

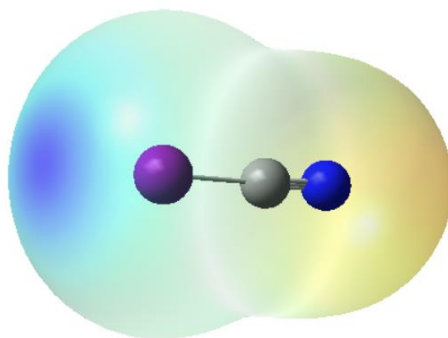


Figure: 1.4. σ -Hole region formed over Iodine in ICN.

1.3. Pi-cloud interaction:

Another type of non-covalent interaction is lone pair- π interactions, which are of great importance for the stabilization of biological macromolecules. These type of Interactions usually occur when pi- cloud over a molecule starts interacting with the lone pair of a nearby situated atom or molecule^[6]. This interaction involves the donation of lone pair electron density to the anti-bonding orbital of pi-cloud. The example of lone pair to pi-interaction is shown below in figure 1.5, where lone pair present in nucleophile interacts with the anti-bonding orbital (pi-clouds) of benzene.

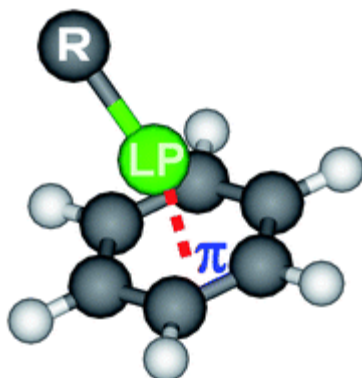


Figure 1.5.: Interaction of Pi-cloud over benzene with lone pair.^[7]

CHAPTER 2

EXPERIMENTAL BASICS

2.1. Matrix Isolation FTIR Spectroscopy:

Infrared Spectroscopy is a technique that uses the infrared region of the electromagnetic spectrum for identification and characterization of chemical substances. The chemical characterizations are usually based on absorption spectroscopy method. The common experimental setup used today for recording an infrared spectrum is the Fourier Transform Infrared Spectrometer (FTIR).^[8]

Matrix Isolation is an experimental technique to study molecules of interest, in an isolated inert environment. The technique involves trapping of sample molecule in a matrix of inert gas, such as argon or nitrogen, at very low temperatures, i.e., ~10 K. The matrix isolated species shows sharp spectral features, owing to minimal intermolecular interactions. Furthermore, the tight cage matrix does not allow any rotational motion of trapped species, thus resulting in sharp features free from spectral congestion. Matrix Isolation FTIR Spectroscopy coupled with *ab initio* calculation has been employed as a useful method for studying molecular conformations, weak intermolecular interactions and complexes and reactive intermediates.

2.1.1. Advantages:

Matrix Isolation is a technique for trapping molecules of interest in an inert matrix at very low temperatures for spectroscopic studies. This method is particularly suitable for preserving reactive, short-lived species and weak complexes in an inert environment. This allows acquisition of spectral data of reactive molecular fragments, conformations and weak complexes, many of which cannot be studied in the gas phase. Using this technique short term reagents such as short radical reagents, radical ions, and intermediate reaction products can be identified using spectroscopic methods.

2.1.2. Properties of a Matrix:

The concentration ratio of matrix to sample is generally 1000:1 which ensures nearly complete isolation of sample, however with the increase in the sample's concentration, the

features of dimers, trimers and various multimers are also observed. The features due to higher clusters are identified by varying its concentrations and temperature. One of the requirements is that at easily achievable temperatures, the sample must have sufficient vapor pressure for deposition.

Also, there are many important properties and characteristic features for inert gas to be used as a matrix.

Inertness: the choice of material used as matrix gas determines the success of the technique. A chemically inert material is preferred as matrix gas to avoid any reaction between the trapped species and matrix molecules. The materials which fulfill the required conditions of chemical inertness are rare gases such as Ar, Kr, Ne, Xe and the inert gas such as N₂, which are therefore commonly used as matrix materials.

Transparency: The matrix material must be highly pure and should be transparent in the spectral absorption range of trapped species, to avoid any spectral interference.

Rigidity: It is required to ensure that no readjustment or diffusion takes place once the matrix is formed. To achieve this condition, the temperature of the matrix must not be greater than one-third of the melting point of the matrix. For example, it is 26K for N₂, 9K for Ne, 29K for Ar, 40K for Kr and 55K for Xe.

Rate of Diffusion: The deposition rate must be controlled to avoid a rise in temperature of the matrix. High deposition rates lead to an increase in the substrate temperature and also lead to a very scattered matrix. According to Moskovits and Ozin, temperature increases with the square of the rate of deposition and increases linearly with the increase of time. The gases mentioned above which are used in matrix form fcc (face-centered cubic) lattice at the working temperature. Depending on the size of the sample molecule, the guest molecule may be trapped in a variety of matrix sites. There also exist interstitial sites like tetrahedral and octahedral voids to accommodate sample molecules, but only small molecules can occupy interstitial sites. The larger molecules will usually be deposited in substitutional sites.

2.2. Matrix isolation FTIR Instrumentation:

2.2.1. CRYOSTAT:

The cryogenic temperature is required to solidify the inert gas to form the matrix and also prevent diffusion of the trapped species. Low temperatures up to 10K are achieved by the compressor with helium as working fluids. Expansion of high pressure He gas cools the

surface of the window.

The cryostat consists of five main parts:

1. Cold head.
2. Helium compressor.
3. Temperature control unit.
4. Optical extension set.
5. Trapping surface.

The closed cycle cryostat used in our setup works on the Gifford McMahon cycle. The expander, commonly known as the cold head or cold finger, is where the Gifford McMahon cycle takes place. It is connected to a compressor through two gas lines for the working fluid (helium) and an electrical power cable. One of the gas lines supplies high-pressure helium gas to the expander, the other gas line returns low-pressure helium gas from the expander. The compressor provides the high pressure. He gas with the necessary flow rate. The vacuum shroud surrounds the cold end of the expander in a vacuum, limiting the heat load on the expander caused by conduction and convection. The radiation shield is actively cooled by the first stage of the expander and insulates the second stage from the room temperature thermal radiation being emitted from the vacuum shroud.

Further, in addition to these major components, the closed cycle cryocooler is often accompanied by several support systems. Typically laboratory systems will have an instrumentation skirt, which provides the vacuum port and electrical feed throws, as well as a temperature controller to measure and adjust the sample temperature. The system also needs electricity, cold water for the compressor, and a vacuum pump for the sample space. Regulation of cold window temperature is attained by using a heater unit, which is mounted near the cold window and couple with closed loop Proportional-Integral-Derivative (PID) controlled. A silicon diode sensor is also placed near a cold window to measure the temperature. Temperature more than 12 K is a prerequisite condition for annealing the matrix, to enhance the diffusion of trapped species thus resulting in complex formation. The cold substrate window is made of potassium bromide as it is infrared transparent. There are four ports that are around this window. One is fitted with quartz for viewing and carrying out UV-visible photo-radiation experiments if required. The opposite port is fitted with an inlet for deposition of matrix gas and sample. The trapping surface can be made of many different materials, but the one that is used should be appropriate for the spectral region that is used; for example, KBr is used for infrared work.

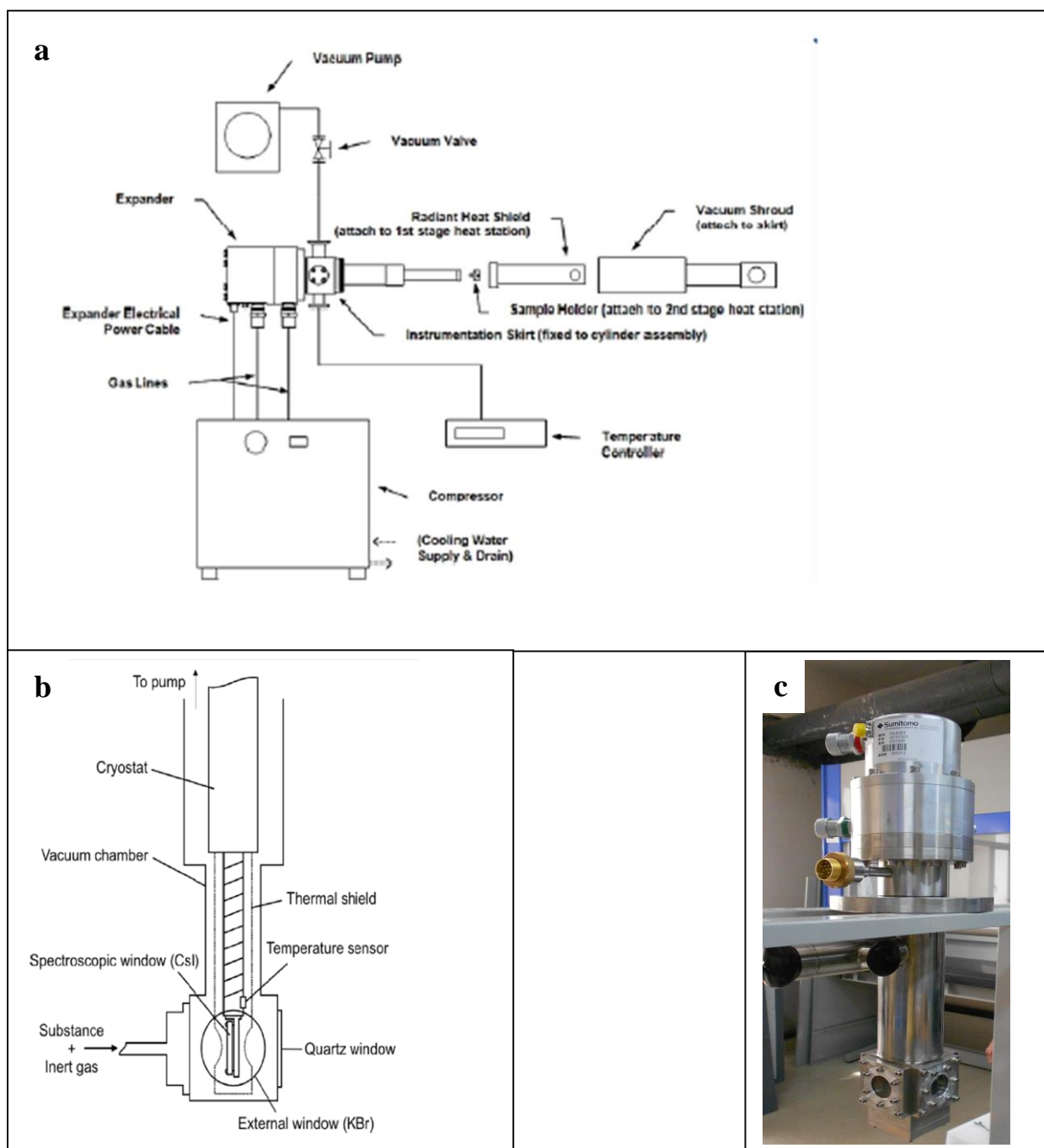


Fig.2.1. (a) The general schematic diagram for the cryosystem assembly; (b) The schematic for the cryostat head mounted on the FTIR Spectrophotometer; (c) Picture of the cryostat mounted in Matrix Isolation set up at IISER Mohali

2.3.2. VACUUM SYSTEM:

A high vacuum condition ($\sim 10^{-6}$ mbar) is an essential prerequisite for matrix isolation method both in terms of supporting the cryogenic setup to attain a low temperature and to ensure that species of interest are trapped without impurities. Oil diffusion pump having a

pumping speed of 280 L / sec is used to evacuate the cryostat. The oil diffusion pump is connected to a rotary pump, which usually has a pumping speed of about 200 L/m.

2.3.3. FTIR SPECTROMETER:

The vibrational spectra of the trapped molecules in the matrix were recorded using a Bruker Tensor 27 FTIR spectrometer. The instrument is usually operated at a resolution of 0.5 cm^{-1} . Typically eight scans are coadded to obtain good signal to noise ratio. All spectra are recorded in the region of $4000\text{-}400 \text{ cm}^{-1}$. After the sample and matrix were deposited at 12K, the spectrum of the matrix isolated species were recorded. After this, the temperature of the matrix was raised to $\sim 25\text{K}$. The matrix was kept at this temperature for about half an hour to one hour using the temperature controller unit. The matrix was then again cooled back to 12K, and a spectrum of the annealed matrix was recorded.

2.3.4. SAMPLE INTRODUCTION SYSTEM:

For compounds which have a lower vapor pressure, the sample is heated to a temperature which ensures adequate vapor pressure to obtain the desired matrix to sample ratio. In cases where the sample has high vapor pressure, the sample is cooled to obtain the desired matrix to sample ratio. The cooling is done using a slush bath of ethanol and liquid nitrogen and maintained at a particular temperature to get the desired vapor pressure.

Single jet system: In a single jet deposition method the sample is taken in a glass container that is connected to a stainless steel mixing chamber. The sample inlet connected to the mixing chamber is opened to allow the sample vapors to fill in the mixing chamber. Then the inert gas is let in and mixed with the sample. This mixture is then streamed through a flow control valve into the vacuum system for deposition on the cold window.

Double jet system: For sample having low vapor pressure, the double jet system of deposition is used. The double jet contains to the nozzle, one for sample deposition and other for matrix gas deposition. The sample nozzle is placed near to cryostat.

The mixing and dilution of the sample molecule with inert gas take place during the process of deposition.

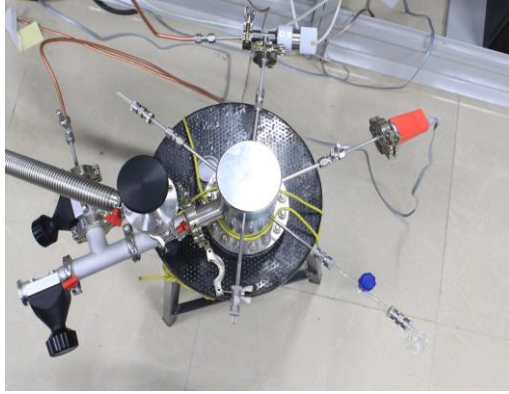


Figure 2.2: Mixing chamber (Stainless steel).

CHAPTER 3

COMPUTATIONAL PROCEDURE

The computational studies are directed towards the computation of molecular structures by ab-initio, quantum mechanical methods. These computational studies are carried out by using the Gaussian-G09 package. Various molecular properties such as optimized geometry, energy, and vibrational frequencies were determined. Presence of weak non-covalent interaction such as hydrogen bonding and secondary interactions were understood using atom in molecule (AIM) analysis. To further support the AIM analysis, natural bonding orbital (NBO) studies were done. These computations methodologies used in this study are briefly discussed below.^[9]

3.1. Computation Methods:

Ab Initio computations:

It signifies calculations from the beginning (inputs are only physical constants). This method attempts to solve the Schrödinger equation given the position of the nuclei and number of electrons which will give the required information of electron densities, energies and different properties related to the system.

DFT: Density function theory is a quantum mechanical modeling method which investigates the electronic structures of many body systems. For calculations in which the energy surface is the quantity of primary interest DFT offers a practical and highly accurate alternative. These methods employ a functional approach, and electronic properties of a system are determined by electron density.

Semi-empirical: Empirical evidence are results of an experiment and hence a unified confirmation. But the semi-empirical methods use some experimental results as inputs. It includes approximations for the various integrals which otherwise would be time-consuming.

Geometry optimizations and frequency calculations are done by using different ab-initio methods. The calculations are primarily done using B3LYP, M062X and MP2 methods together with different basis sets. The basis set used is DGDZVP, as it includes a pseudopotential for iodine compounds. It generally gives better agreement for X-I bond lengths. The full electron basis also allows adequate calculations of the quadrupole

coupling constant of Iodine and are generally characterized by smaller computing time.

3.1.1. Ab-initio studies (Related methods):

1. **B3LYP (Becke-Lee-Yang-Parr) Method:** It is a widely used DFT method for ab-initio electronic structure calculations. This method shows significant improvement over the Hartree-Fock (HF) method. It includes the electron spin densities and their gradients. The B3LYP includes the Becke three parameter non-local exchanges functional with the non-local correlation of Lee, Yang, and Parr.
2. **M06:** These are hybrid DFT methods which are developed by Scuseria and Staroverov's keeping six strategies in mind that have been widely used for making density functions. The six strategies include: 1.local spin density approximation (LSDA). 2. Density gradient expansion. 3. Constraint satisfaction. 4. Modeling the exchange correlation hole. 5. Empirical fits. 6. Mixing Hartree-Fock and approximate DFT exchange. Here the 2X refers to the percent of HF exchange which roughly amounts to 54%. It is recommended to be applied to problems including non-covalent interactions.
3. **MP:** (Moller Plesset Perturbation Theory) this is a post-HF method which improves on the Hartree-Fock method by adding electron correlation effects, using Rayleigh-Schrödinger perturbation theory (RS-PT), usually to second (MP2), third (MP3) or fourth (MP4) order. But it must be noted here that the higher orders of theories may not necessarily be convergent.

3.2 ENERGY CALCULATIONS:

3.2.1. Geometry Optimization:

Geometry optimization or Minimization of energy is an important step to find a geometry, for which the net interatomic force on each atom is close to zero, and the position on the potential energy surface (PES) is a stationary point. Optimization of a molecule sometimes leads to problems like convergence towards a local minimum instead of global minima. These problems can be overcome by giving different input geometry to obtain the lowest energy structure which is the global minima. The local and global minima on a potential energy surface are shown in figure 3.1:

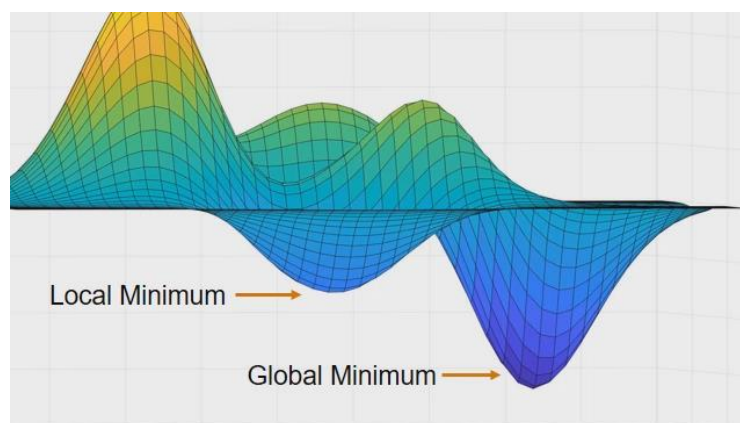


Figure 3.1: Local and global minimum at potential energy surface.^[10]

The geometry optimization begins with the guess molecular structure, specified in the input file and steps along the potential energy surface. The information derived in a given step of optimization is used to identify the direction in which the next step is taken.

Optimization of ICN-H₂S complexes was performed at different levels of theory such as B3LYP, M06-2X, MP2 using DGDZVP basis set. Vibrational frequency calculations of optimized complexes were done at the same level of theory to ensure that the complex structures did correspond to the minima of the potential energy surface. These frequency values are also used for the comparison with experimental spectra. The scaling factor was calculated by assigning the strongest observed in the experiment with the most intense computed wavenumber. The computed scaled frequencies are then used to simulate the vibration spectra.

3.2.2. STABILISATION ENERGIES:

Raw energy:

The stabilization energies of molecular complexes are calculated using the following formula:

$$\Delta E = E_{AB} - (E_A + E_B)$$

Where E_A , E_B , and E_{AB} describes the energy of monomer A, monomer B, and Complex. The negative value of ΔE implies that the energy of monomers is more than that of complex and thus the complex obtained is energetically stable then monomer species. The stabilization energy of complex was calculated using the raw electronic energy, ZPC (zero points corrected) energy and BSSE (basis set superposition error) corrected energy.

Zero Point Energy (ZPE) [11]:

Zero Point Energy is generally described as the difference between the lowest possible energy that a quantum mechanical system and classical minimum energy of the system.

The zero points vibrational energy ZPVE (or ZPE) is the vibrational motion of molecular systems even at 0 K and is calculated for a harmonic oscillator model as a sum of contributions from all i vibrational modes of the system:

$$\text{ZPVE} = \sum_i 0.5 hc \tilde{\nu}_i$$

The zero point energy correction is the sum of total electronic energy and zero-point energy.

$$E_{\text{tot}} = E_{\text{ZPE}} + E_{\text{elec}}$$

Basis Set Superposition Error (BSSE) [12]:

When atoms of two interacting molecules or a different part of the same molecule approach one another, their basis set overlaps. Due to this effect, the monomer takes function from the nearby components which effectively increase its basis set and improving the calculation of energy. If the total energy of the system is minimized as a function of its geometry, then the short range energies from the mixed basis sets must be compared with the long-range energies from the unmixed sets, and this mismatch introduces an error. These errors are more pronounced for smaller basis-sets. The commonly used method to correct the BSSE correction is by counterpoise correction (additional keyword: counterpoise=2) proposed by Boys and Bernadi. In this the energy difference is obtained as follows:

$$\Delta E = E_{\text{AB}}(\text{AB}) - \{E_{\text{A}}(\text{AB}) + E_{\text{B}}(\text{AB})\}$$

Where, $E_{\text{A}}(\text{AB})$ = Energy of monomer A using basis set AB,

$E_{\text{B}}(\text{AB})$ = Energy of monomer B using basis set AB,

$E_{\text{AB}}(\text{AB})$ = Energy of complex using basis set AB.

3.3. ANALYSIS OF THE DIFFERENT WEAK COMPLEXES:

3.3.1. AIMS (Atoms In Molecules) Methodology ^[13]:

The nature of interaction in the weakly bounded complex is understood by performing atom in molecule (AIM) analysis. This involves analysis of the electron density topology of molecular complexes. The wave function corresponding to the optimized geometry is obtained using Gaussian-09. These electron density plots give critical points, charge density ($\rho(r_c)$) at critical points and Laplacian of charge density ($\nabla^2\rho(r_c)$) which is the trace of hessian of ρ . The charge density has a definite point in space. Each topological feature of $\rho(r_c)$, where it is a maximum, minimum or a saddle point has associated with it in a space called the critical point where the first derivative of $\rho(r_c)$ vanishes. The second derivative at this function determines whether this point is maximum or minimum. The critical points (CP) are labeled by giving the values (ω, σ) where σ is algebraic sum of signs of eigenvalues and ω is rank of the critical point (number of non-zero eigenvalues). A (3,-1) corresponds to the bond between two atoms, (3,+1) CP to ring, (3,+3) CP to a cage and (3,-3) CP to a maximum. The number of critical points of all types which can coexist in a system with a finite number of nuclei is seen by Poincare Hopf relationship:

$$\mathbf{n-b+r-c=1}$$

Where n is a number of nuclei, b is the number of bond critical points, r is the number of ring critical points and c is the number of cage critical points.

Laplacian of charge density may be positive or negative but is usually of the same order of magnitude of ρ then the interaction is of shared type or covalent type typically. For closed shells interactions such as Van der Waal's interaction, hydrogen bond complexes and ionic systems the charge density at BCP is small, and Laplacian of charge density is positive.

3.3.2. Natural Bonding Orbitals (NBO)^[14]:

Natural bonding orbital (NBO) analysis is done to identify the orbitals delocalization interaction involved in a weakly bonded complex. In NBO analysis a given wave function is transformed into a localized form which corresponds to a Lewis structure. The input atomic orbital basis set is transformed via natural atomic orbital (NAO's) and natural hybrid orbitals (NHO's) into a set of natural bonds orbital (NBOs). Thus this results in giving a Lewis picture of the molecule where 2-centered bonds and 1-centered lone pairs are localized which can interact strongly with each other. Here, an empty orbital can act as acceptor and bonded, or lone pair can act as a donor. These interactions can hence be strengthened or weaken the bonds. Electron delocalization on Lewis structure depicts the

donor-acceptor interactions. The extent of delocalization of electron density depends upon the relative energy of orbitals and the orbital symmetry of donor and acceptor.

CHAPTER 4

RESULTS AND DISCUSSIONS

In ICN, the nitrogen is the most electronegative atom and results in the strong dipole. It can be therefore anticipated that dipole-dipole interaction will result in a complex with H₂S. At the iodine end of the ICN molecule, the electron attaining CN group results in the formation of a σ -hole represented by electrostatic potential as shown in Figure 4.1.

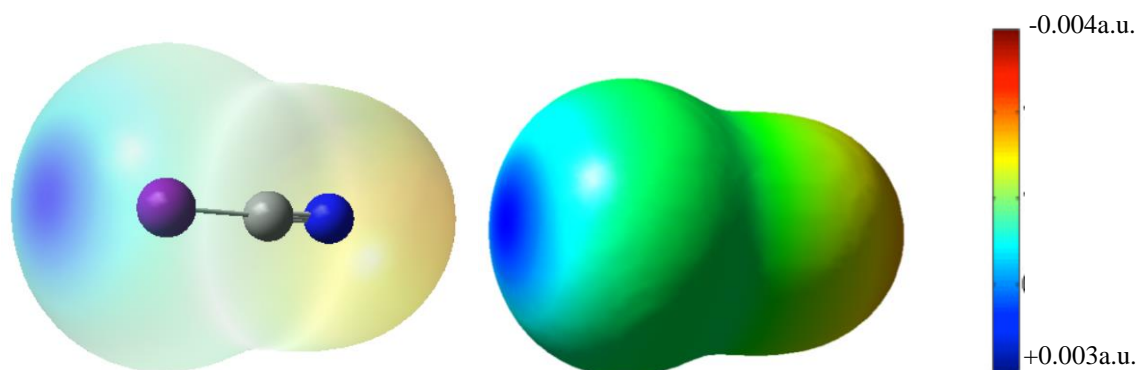


Figure 4.1.: The σ -hole character of ICN.

The blue region over the surface show regions of positive potential and orange-red cloud over nitrogen depicts the region of negative charge. The σ -hole character of ICN helps in the formation of halogen bonded complex.

4.1. H₂S-ICN COMPLEXES:

Interaction of H₂S with ICN forming hydrogen-bonded complexes between these two precursors were studied using ab initio computations and three different 1:1 complexes were found, each displaying three different non-covalent interactions:

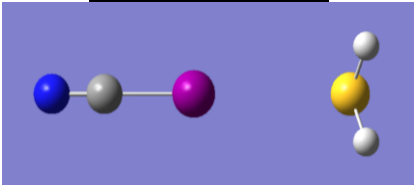
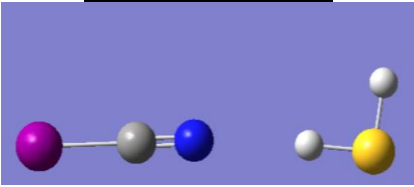
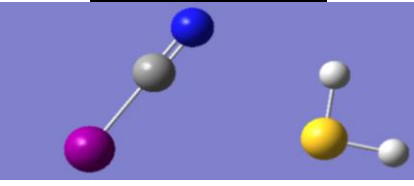
- 1) Halogen interacting with S in H₂S. (Halogen Interaction)
- 2) N of ICN interacting with H in H₂S. (Hydrogen Interaction)
- 3) π -cloud of CN interacting with S in H₂S. (Pi-Cloud Interaction)

4.1.1. Computational Results:

The relative stability of the three optimized structures of ICN-H₂S complexes are studied on the basis of their interaction energies as shown in Table 4.1. The interaction energy calculations are done using Gaussian 09 on different levels of theory: B3LYP, M06-2X and MP2 methods together with DGDZVP basis set. This basis set was chosen to accommodate iodine in our calculations. The structures of optimized geometries of these complexes were

same at all levels of calculation used. Optimized geometries for monomers (H₂S and ICN) were also computed at all the levels, which were then used to calculate the interaction energy of complexes.

Table 4.1.: Energies for halogen, hydrogen and pi-cloud interaction at different levels of theories.

<u>GEOMETRIES</u>	<u>Interaction Energy</u> <u>Raw/BSSE/ZPE</u>	
<p><u>Halogen Interactions</u></p> 	B3LYP/DGDZVP	-3.8/-3.4/-2.4
	MO62X/DGDZVP	-4.6/-4.2/-3.2
	MP2/DGDZVP	-3.8/-2.6/-2.5
<p><u>Hydrogen Interaction</u></p> 	B3LYP/DGDZVP	-2.1/-1.7/-0.9
	MO62X/DGDZVP	-2.4/-2.0/-1.1
	MP2/DGDZVP	-2.7/-1.9/-1.5
<p><u>Pi-Cloud Interaction</u></p> 	MO62X/DGDZVP	-2.5/-2.2/-1.2
	MP2/DGDZVP	-2.3/-1.3/-1.2

The energies calculated are corrected for BSSE and ZPE. It can be inferred that the halogen bonded complex is the most strongly bound of the three complexes and thus global minimum for ICN-H₂S system. It is also seen that the interaction energies of hydrogen-bonded complex and the Π -cloud structure are similar.

The frequency calculations were also performed at M06-2X/DGDZVP level of theory. It was seen that all the computed harmonic frequencies were positive and thus all geometries of ICN-H₂S complexes obtained, are indeed minima on the potential energy surface.

4.1.2. Atom in Molecule (AIM) Analysis:

Atom in Molecule Analysis at the M06-2X/DGDZVP level is done to understand the nature of interaction in these complexes as shown in figure 4.2. The (3,-1) bond critical points (BCP) associated with the complexes were located. The BCPs are located for the Halogen

and Hydrogen bonded complexes. However, no BCP was seen between the Π -cloud of CN and the S atom, for Pi-cloud interaction complex.

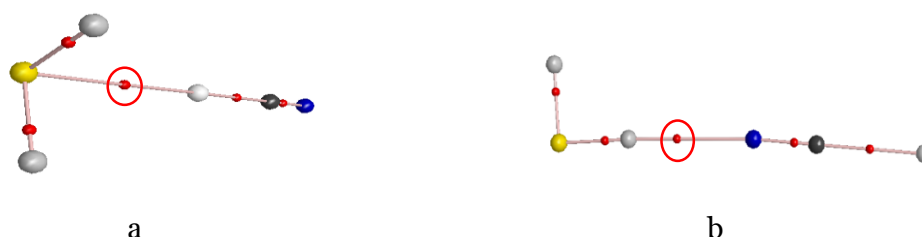


Figure 4.2: Electron density topologies a) Halogen Interaction. b) Hydrogen Interaction. (BCPs corresponding to these interactions are circled).

The values of charge density ($\rho(r_c)$) and Laplacian of charge density ($\nabla^2\rho(r_c)$) at the bond critical points for halogen and hydrogen bonded interactions are listed in Table 4.2.

Table 4.2: AIM results showing the charge density and Laplacian for interactions on BCP at M06-2X/DGDZVP level.

INTERACTION	Charge Density at B.C.P ($\rho(r_c)$)	Laplacian ($\nabla^2\rho(r_c)$) at B.C.P
Hydrogen bond	0.012 a.u.	0.042 a.u.
Halogen bond	0.012a.u.	0.034 a.u.

AIM analysis was also done on the π cloud interaction complex at the M06-2X/DGDZVP level. However, BCP between the π cloud of CN and the Sulfur atom of H₂S was absent. Thus, Natural bond orbital (NBO) analysis was then performed on all the complexes to understand the donor-acceptor orbital interactions, responsible for hydrogen-bonded structures in the ICN-H₂S complexes.

Natural Bonding Orbitals (NBO) Analysis:

NBO analysis was performed at the B3LYP, M06-2X, and MP2 methods using *DGDZVP* basis set. Table 4.3 lists some important donor and acceptor orbital interactions for ICN-H₂S together with their second order perturbation energy denoted by E(2). This study shows that in the case of halogen bonding, the electron donor is sulfur in H₂S whose lone pair interacts with anti-bonding orbital of I-C bond.

Table 4.3: NBO analysis showing some important donor and acceptor orbital interactions for ICN-H₂S complexes. E denotes delocalization energy in kcal/mol for each interaction. (Unit 1 is ICN and Unit 2 is H₂S).

	Donor NBO (i)	Acceptor NBO (j)	E (kcal/mol)
<i>B3LYP</i>			
HALOGEN BONDING	from unit 2 to unit 1		
	(n2) S	/(σ*) I - C	5.43
HYDROGEN BONDING	from unit 1 to unit 2		
	(n1) N	/(σ*) S - H	2.71
<i>M062X</i>			
HALOGEN BONDING	from unit 2 to unit 1		
	(n2) S	/(σ*) I - C	6.36
HYDROGEN BONDING	from unit 1 to unit 2		
	(n1) N	/(σ*) S - H	2.94
PI-CLOUD	from unit 2 to unit 1		
	(n2) S	/(Π ₂ *) C - N	0.89
<i>MP2</i>			
HALOGEN BONDING	from unit 2 to unit 1		
	(n2) S	/(σ*) I - C	5.82
HYDROGEN BONDING	from unit 1 to unit 2		
	(n1) N	/(σ*) H - S	2.94
PI-CLOUD			

In the case of hydrogen-bonded complex, the lone pair on the nitrogen atom in ICN donated electron density to the anti-bonding of S-H in H₂S. It must also be noted that NBO analysis showed the donation of electron density from the lone pair of Sulfur atom to the bonding orbital of CN bond in ICN. This clearly points out presence of weak Π-cloud interaction, for which, however, AIM analysis did not indicated the bond critical point.

4.1.3. Experimental details:

ICN was loaded in a glass bulb inside a glove bag to avoid the contaminations due to

moisture. To create inert environment inside a glove bag, Ar gas is continuously passed through it. The matrix was deposited by introducing into the vacuum chamber the mixture of ICN, H₂S and Ar. The components are introduced using double jet nozzle. Through one nozzle, a mixture of H₂S and Ar gas is passed (which are mixed in ratio (2.5:1000) and through a second nozzle ICN was passed. The ICN sample was maintained at ~0°C for 30 minutes prior to the deposition using ice bath. At this temperature the vapor pressure of the ICN sample is sufficient to ensure isolation in the Ar matrix and to avoid the formation of multimers. Thus ICN together with H₂S and Ar mixture was then deposited for about an hour, at the KBr window kept at 12K. After deposition, the spectra of the matrix deposited was recorded at 12K. Further, the temperature of matrix was raised from 12K to 25K for 15 minutes to encourage diffusion of the trapped species and enable complex formation. The spectra of the matrix was thus annealed and then again recorded by re-cooling the matrix to 12 K. Experiments were also performed with ICN maintained at -20°C to determine the concentration dependence of complex formation.

Experimental results:

The experimental spectra features were assigned using the scaled computed frequencies for ICN-H₂S complexes. The scaling factor was calculated by dividing experimentally observed most intense feature with the feature computed to have highest intensity in the appropriate spectral region. The computed scaled frequencies are then used to simulate the vibration spectra using SYNSPEC software. The scaled computed vibrational frequencies for ICN-H₂S complexes bound by halogen and hydrogen bond interaction at the M06-2X/DGDZVP level are given in table 4.4.

Table 4.4: Computed scaled vibrational frequencies (in cm⁻¹) with their shifts calculated as $\nu_{\text{complex}} - \nu_{\text{monomer}}$ at M06-2X/DGDZVP level.

		ASYMMETRIC MODE (H ₂ S)	SYMMETRIC MODE (H ₂ S)	CN STRECH (ICN)
	SCALING FACTOR	0.9587	0.9575	0.9222
MONOMER	Scaled Frequency	2648.0	2624.0	2170.5
HALOGEN COMPLEX	Scaled Frequency	2651.7	2628.0	2164.3
	Shift	3.7	4.0	-6.2
HYDROGEN COMPLEX	Scaled Frequency	2642.6	2611.9	2173.5
	Shift	-5.4	-12.1	3.0

The experimental features in the FTIR spectra was observed experimentally in two regions; one in the S-H stretch (symmetric and asymmetric stretch) that lie in the range of 2700-2600 cm^{-1} and the other in CN stretch region of ICN which lies in the range 2200-2150 cm^{-1} . Peaks in both of these regions were analyzed and the discussion is presented in the following section.

S-H Region:

Feature observed at 2624.6 cm^{-1} corresponds to H_2S symmetric stretch in the monomer^[15]. When ICN was co-deposited with H_2S in Ar matrix, new feature was observed at 2609.7 cm^{-1} . This feature shows a red shift of 14.9 cm^{-1} from the S-H symmetric stretch in H_2S monomer, on complex formation (Figure 4.3). This shift of 14.9 cm^{-1} is in good agreement with the computed shift of 12.1 cm^{-1} for the ICN- H_2S hydrogen bonded complex as given in table 4.4.

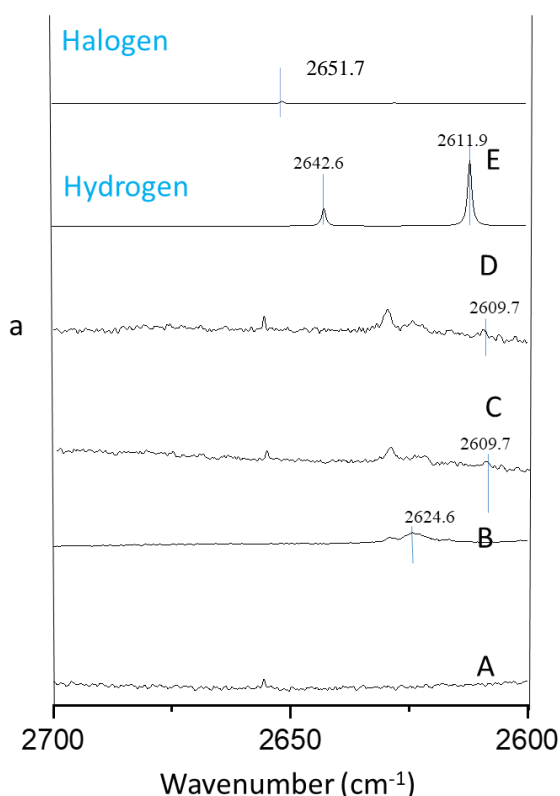


Figure 4.3: FTIR spectra of H_2S in the symmetric stretch region. Experimental spectrum of A) ICN in an Ar matrix, B) H_2S in an Ar matrix, C) ICN- H_2S in Ar (ICN at 0°C) at 12K, D) ICN- H_2S in Ar annealed at 30K, Computed spectra of ICN- H_2S E) Hydrogen bonded complex, F) Halogen bonded complex.

C≡N Stretch Region:

Strong feature was observed at 2170.5cm^{-1} which is due to CN stretch in ICN monomer. On complex formation new features were observed at 2171.5 cm^{-1} , blue shifted by 1.0 cm^{-1} from the same mode in uncomplexed ICN. ICN. This feature matches with the computed feature (2173.5 cm^{-1}) blue shifted by 3.0 cm^{-1} , for the hydrogen bonded complex between ICN and H_2S .

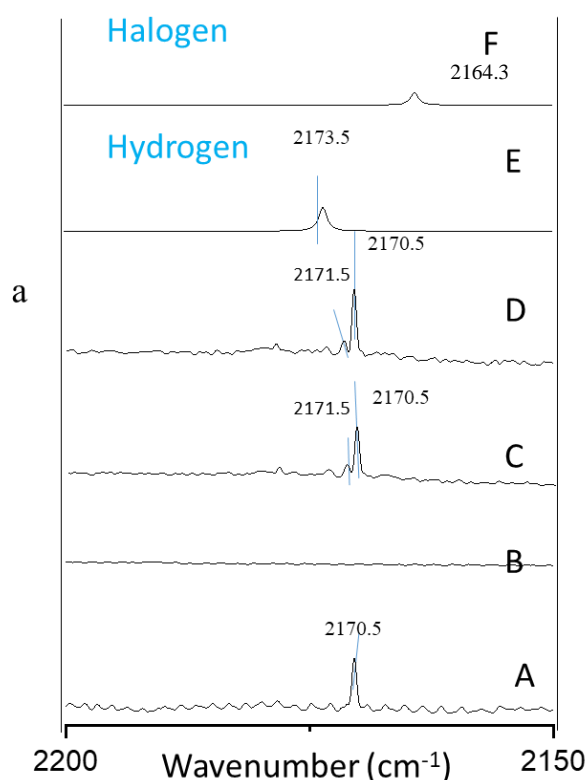


Figure 4.4: FTIR spectra of ICN in the CN stretch region. Experimental spectrum of A) ICN in an Ar matrix, B) H_2S in an Ar matrix, C) ICN- H_2S in Ar (ICN at 0°C) at 12K, D) ICN- H_2S in Ar annealed at 30K, Computed spectra of ICN- H_2S E) Hydrogen bonded complex, F) Halogen bonded complex

Our work on ICN- H_2S system shows that complex involving S-H...N hydrogen bonded interaction was observed in our matrix experiments. There was no evidence of the formation of the global minimum halogen bonded complex in the experiments.

4.2. ICN- CH_3SH COMPLEXES:

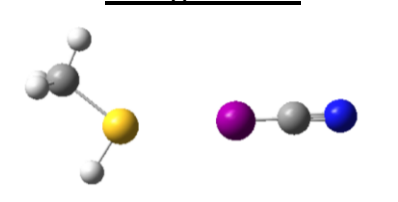
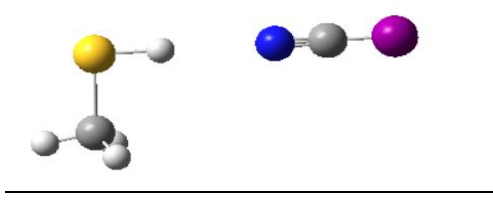
ICN hydrogen bonded complexes with CH₃SH were also studied, in order to understand the effect of an electron donating group, CH₃. These interactions were seen to see the effect of a bulkier group attached to Sulfur. Computationally two geometries for these interactions were obtained and no Pi-cloud interaction was optimized in this system. Thus the two structures were obtained at M06-2X/DGDZVP level of theory:

- 1) Halogen interacting with S in CH₃SH.
- 2) N of ICN interacting with H in CH₃SH.

4.2.1. Computational Studies:

The interaction energy calculations for the optimized ICN-CH₃SH complexes were calculated at different levels of theories i.e. B3LYP, M062X and MP2 and basis set for which is again DGDZVP. The values for which are shown in the table 4.5:

Table 4.5: Interaction energies for Halogen and Hydrogen bonded ICN-CH₃SH complexes at different levels of theories.

<u>Complexes</u>	<u>Interaction Energy (in kcal/mol)</u> <u>Raw/BSSE/ZPE</u>	
<p style="text-align: center;"><u>Halogen Bond</u></p> 	B3LYP/DGDZVP	-5.0/-4.4/-3.8
	M06-2X/DGDZVP	-6.0/-5.4/-4.9
	MP2/DGDZVP	-5.1/-3.5/-4.1
	MP4/DGDZVP	-5.2/-3.5/-4.0
<p style="text-align: center;"><u>Hydrogen Bond</u></p> 	B3LYP/DGDZVP	-1.6/-1.3/-0.7
	M06-2X/DGDZVP	-1.2/-0.7/0.2
	MP2/DGDZVP	-2.8/-1.8/-1.9
	MP4/DGDZVP	-2.8/-1.8/-1.7

The energies calculated were separately corrected for BSSE and ZPE. It is clear from Table 4.5 that halogen bonded complex is the most stable structure constituting the global minimum with BSSE corrected energy of -5.4 kcal/mol at M06-2X/DGDZVP level. The hydrogen bonded complex was found less stable with BSSE corrected energy of -0.7 kcal/mol at the same level of calculation.

4.2.2. Atom in Molecule (AIM) Analysis:

From AIM analysis, Bond critical points (BCP) which are given by $(-3,1)$ associated with the ICN-CH₃SH complexes were located. The BCPs are located in Halogen and Hydrogen bonded complexes. In addition, a ring critical point $(3,+1)$ is also located in hydrogen bonded CH₃SH-ICN interaction since nitrogen atom in ICN being a highly electronegative will also interact with the hydrogen atom of the methyl group in CH₃SH, as shown in figure 4.5. The values of charge density ($\rho(r_c)$) and Laplacian ($\nabla^2\rho(r_c)$) at the BCPs in the ICN-CH₃SH complexes are shown in Table 4.6.

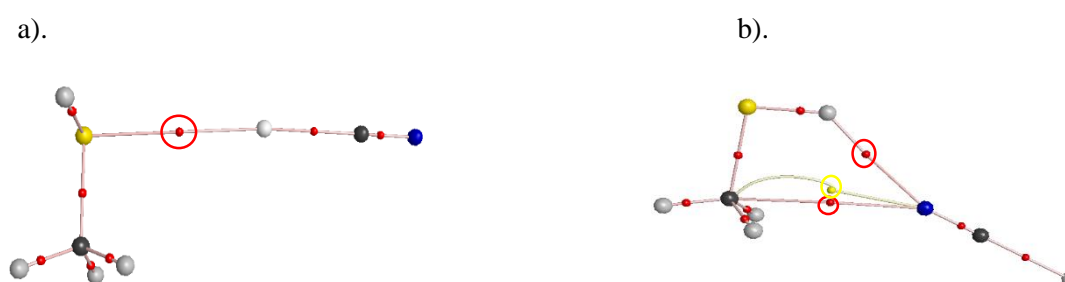


Figure 4.5: Electron density topologies for the ICN-CH₃SH a) Halogen bonded and b) Hydrogen bonded complexes at the M06-2X/DGDZVP level.

Table 4.6: Charge Density and Laplacian for Interactions at M06-2X/DGDZVP level of theory (in a.u.).

INTERACTION	Charge Density at BCP ($\rho(r_c)$)	Laplacian ($\nabla^2\rho(r_c)$) at BCP
Hydrogen Interaction 1. S-H...N	0.009	0.031
2. C-H...N	0.006	0.024
Halogen Interaction	0.014	0.035

4.3. COMPARISONS:

The results for ICN-H₂S complexes, were compared with the earlier studied ICN-H₂O complexes^[16] to analyze the differences in interactions and extent of bonding (Halogen and Hydrogen) with the change of compound. The comparison of interaction energies for both

halogen and hydrogen complexes were made to identify the differences between H₂O and H₂S complexation with ICN shown in table 4.7. It is clearly seen that in both cases same trend is followed indicating that the halogen interaction was found to be stronger than the hydrogen interaction. In addition, ICN-H₂O complexes were more stable than ICN-H₂S complexes and the energy difference between the halogen and hydrogen bonded complex is almost double in ICN-H₂O complexes relative to ICN-H₂S system.

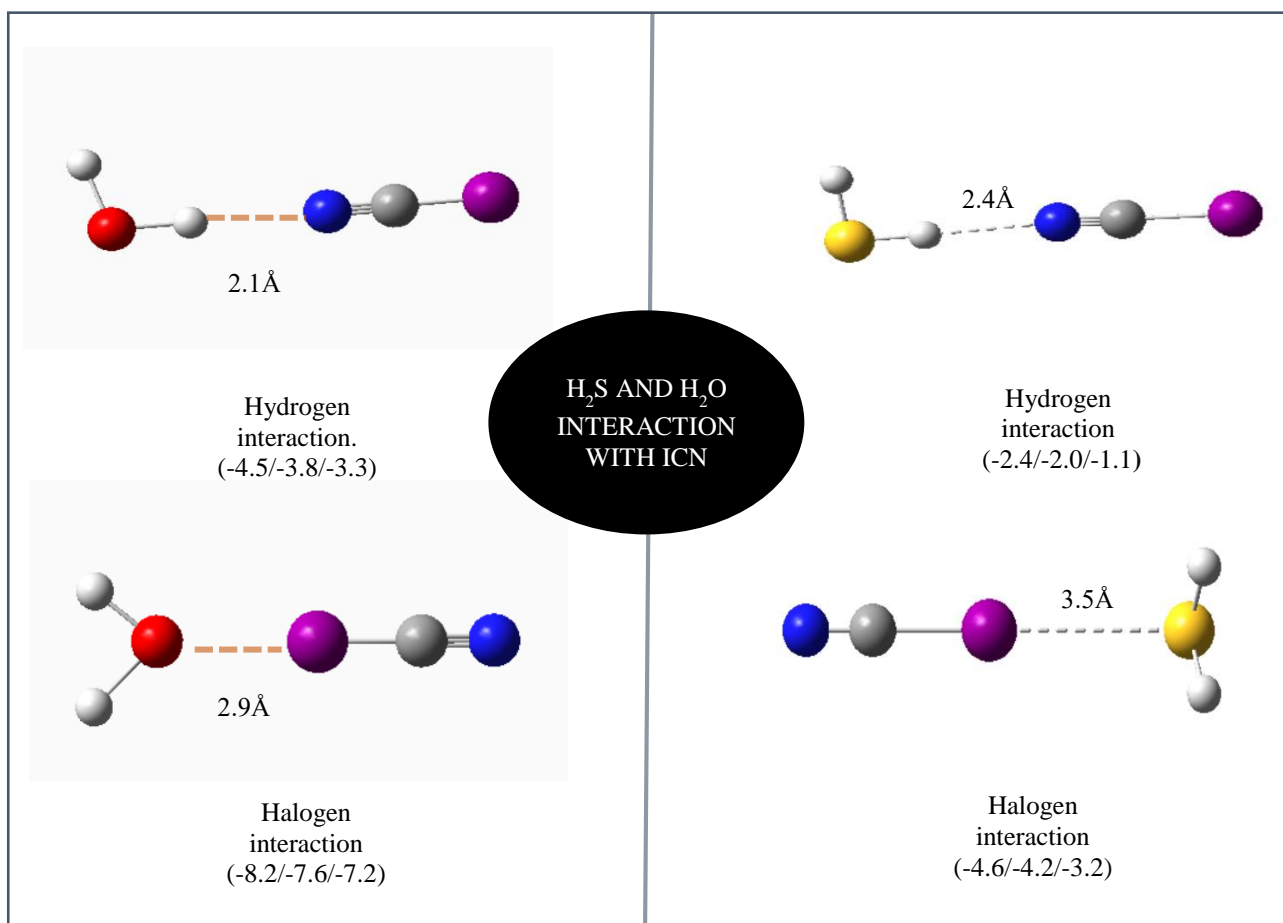


Figure 4.6: Comparison of ICN-H₂O and ICN-H₂S system with their RAW/ZPE corrected/BSSE corrected interaction energies in kcal/mol at M06-2X/DGDZVP level.

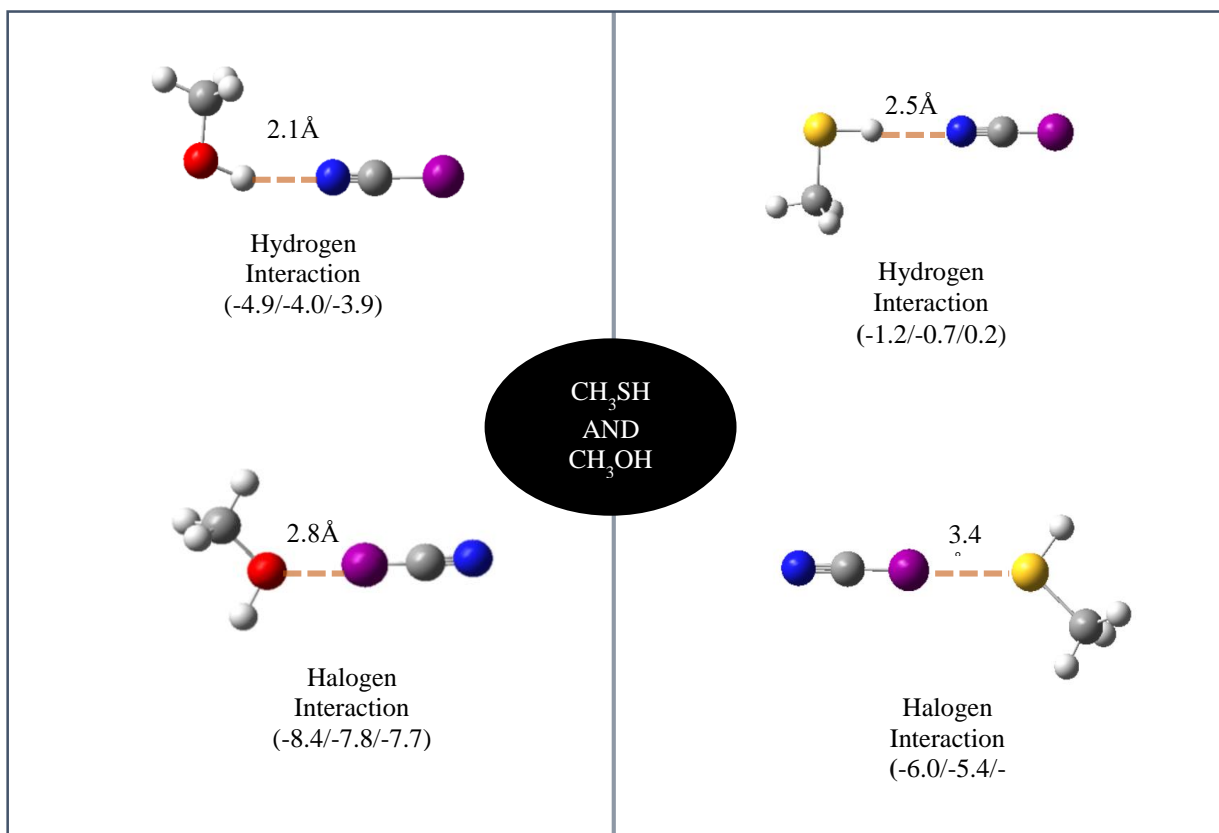


Figure 4.7: Comparison of ICN-CH₃OH and ICN-CH₃SH system with their RAW/ZPE corrected/BSSE corrected interaction energies in kcal/mol at M06-2X/DGDZVP level.

Similarly, ICN-CH₃OH and ICN-CH₃SH complexes were compared as shown in Table 4.8. It can be deduced that again same trend interaction of energy is followed since halogen bonded complex is more stable than the hydrogen bonded complex. In addition, ICN-CH₃OH complexes are more stable than ICN-CH₃SH complexes. One contrasting point to notice here is that the energy difference between halogen and hydrogen bonded complex in ICN-CH₃OH system is slightly less relative to that in ICN-CH₃SH complexes.

CHAPTER 5

CONCLUSION

In this thesis work, ab initio computations at the M06-2X/DGDZVP level, have located three types of non-covalent interactions between ICN and H₂S. These interactions include Halogen bonding (Cl...S), Hydrogen bonding (SH...N) and Pi-cloud Interaction (π ...S). Our matrix isolation FTIR experiments showed presence of only the Hydrogen bonded complex. There was no evidence of the formation of the Halogen bonded and Pi- cloud interaction complex, in our experiments. In addition, interactions between CH₃SH and ICN were also studied computationally, for which two structures were optimized as minima on the potential energy surface. One complex was bound by the Halogen interaction and other by dual hydrogen bonded contacts: SH...N and CH...N interaction.

The structure involving π cloud of CN interacting with S atom did not optimize for the ICN-CH₃SH system. In both ICN-H₂S and ICN-CH₃SH system, Halogen bonded complex was computed to be more stable than the Hydrogen bonded complex. Whereas from the interaction between CH₃SH and ICN it can be concluded that Sulfur compounds are more sensitive toward the functional group attached and it can bring change to type of bond formed or the extent of bond formed (Halogen or Hydrogen). The computations were done using M06-2X level of theory and DGDZVP basis set.

Experiments done for the ICN-H₂S system using Matrix Isolation FTIR

Spectroscopy, showed evidence for the hydrogen bonded complex in both the H₂S symmetric stretch and the CN stretch region. However, interestingly no experimental evidence for halogen bonded complex was found, even though this complex represented the global minimum. It is possible that matrix interactions may have a role to play in the local minimum being observed as against the global minimum. Our experiments also indicated the possible presence of higher complexes such as ICN-(H₂S)₂. However, computations will have to be performed for the higher complexes to make firm assignment. Future aspects: More experiments using different matrix gas (N₂, Xe) can be done to study the role of the matrix interaction.

Bibliography

1. Dipole-Dipole interaction by libretexts.org.
2. Lee Brammer, Guillermo Mínguez Espallargas and Stefano Libri, Combining metals with halogen bonds, *CrystEngComm*, 2008,**10**, 1712-1727.
3. The nature of water by socratic.org
4. Cavallo, G., Bruce, D. W., Terraneo, G., Resnati, G., Metrangolo, P. From Molecules to Materials: Engineering New Ionic Liquid Crystals Through Halogen Bonding. *J. Vis. Exp.* (133), e55636, doi:10.3791/55636 (2018).
5. Halogen bond by Wikipedia.
6. Pi interaction by Wikipedia.
7. Tidido J. Mooibroek, Patrick Gamez and Jan Reedijk, Lone pair- π interactions: a new supramolecular bond?, *CrystEngComm*, 2008,**10**, 1501-1515.
8. Lester Andrews, Encyclopedia of Spectroscopy and Spectrometry (Second Edition), 1999, Pages 1479-1483.
9. Computational chemistry by Wikipedia.
10. Gutmann, H.-M. *A radial basis function method for global optimization*. Journal of Global Optimization 19, Issue 3, 2001, pp. 201–227.
11. Simone Morpurgo, Giorgio O. Morpurgo, Advances in quantum chemistry, Volume 36, 2000, Pages 169-183.
12. Counterpoise by Gaussian.com
13. G. Henkelman, A. Arnaldsson, and H. Jónsson, A fast and robust algorithm for Bader decomposition of charge density, *Comput. Mater. Sci.* 36, 354-360 (2006).
14. Natural bond orbital by researchgate.net.
15. *J. Phys. Chem. A* 1999, 103, 679-685 .
16. Computational data for H₂O-ICN experiments was taken from Amala's Master thesis "ICN- A treasure mine for non-covalent interactions" for comparisons.

